Supplementary Information:

Structure and electronic transport in graphene wrinkles

Wenjuan Zhu*, Tony Low, Vasili Perebeinos, Ageeth A. Bol, Yu Zhu, Hugen Yan,

Jerry Tersoff and Phaedon Avouris*

IBM Thomas J. Watson Research Center, Yorktown Heights, NY 10598, USA

1. Maximum height estimate of the *standing collapsed wrinkle*.

To estimate the maximum height, we assume that the wrinkle has a fixed amount of material (i.e. no sliding of graphene along the surface), and that it adopts the minimum-energy morphology. We therefore need to compare energies of the different structures for a fixed amount of excess graphene in the wrinkle. First, we estimate energy of the *folded wrinkle*. As illustrated in Fig. S1, the structure of *folded wrinkle* consists of the right and left bulb-shaped curves with similar radiuses and a flat trilayer region. The right bulb we approximate by a pair of arcs, concave and convex. The two left bulbs are approximated by the arcs of the same angles, with radiuses being different by the van der Waals distance h separating graphene layers. The trilayer region has length λ, and the bilayer has length $\lambda+\xi$. The base is approximated by arcs of angle $\pi/2$ and radius R_b. The energy of the *folded wrinkle* in this model is given by:

$$
\begin{aligned}
E_f = {} & \frac{\kappa}{2}\left(\frac{\pi}{R_b} + \frac{\theta_1}{R_1} + \frac{\theta_1}{R_1+h} + \frac{\theta_2}{R_2} + \frac{\theta_2}{R_2+h} + \frac{\theta_3}{R_3} + \frac{\theta_4}{R_4} \right) \\
& -\beta\left(\theta_1\left(R_1+\frac{h}{2}\right) + \theta_2\left(R_2+\frac{h}{2}\right) + 2\lambda + \xi \right) \\
& +\beta_{sub}\left(2R_b+h\right)
\end{aligned}
\tag{1}
$$

where κ is graphene bending stiffness and β is van der Waals adhesion energy. The first term reflects the bending energy, the second term reflects adhesion energies of the bilayer and trilayer regions, and the last term reflects the adhesion energy cost to peel off

graphene from the substrate. We will use $\beta_{sub}=\beta$. The excess length is defined as the length of the graphene fold minus the length of the flat substrate and it is given by:

$$L = \pi R_b + \theta_1 (2R_1 + h) + \theta_2 (2R_2 + h) + 2\lambda + \xi + \theta_3 R_3 + \theta_4 R_4 - (2R_b + h) \qquad (2)$$

where relationships between the angles and radiuses are determined by the geometric constraints, see Fig. S1: $\xi = R_4 \sin \theta_4 - R_3 \sin \theta_3$, $\theta_1 - \theta_2 = \pi/2$, $R_1 \sin \theta_1 + R_b = h + (R_2 + h)(1 - \cos \theta_2)$, $\theta_3 - \theta_4 = \pi$, $R_3 (1 - \cos \theta_3) = h + R_4 (1 - \cos \theta_4)$. Minimization of energy in Eq. (1) with respect to the five variational parameters R_b, R_1, θ_1, R_3, θ_3 for a fixed excess length L from Eq. (2) gives the energy of the fold as a function of L.

Similarly, we can estimate the energy of the *standing collapsed wrinkle* geometry, shown in Fig. S2:

$$E_{sc} = \frac{\kappa}{2} \left(\frac{\pi}{R_b} + \frac{2\theta_1}{R_1} + \frac{2\theta_2}{R_2} \right) - \beta\lambda + \beta_{sub} (2R_b + h) \qquad (3)$$

The excess length here is given by:

$$L = \pi R_b + 2\lambda + 2\theta_1 R_1 + 2\theta_2 R_2 - 2R_b - h \qquad (4)$$

where $\theta_1 = \theta_2 + \pi/2$, $R_1 \sin \theta_1 = h/2 + R_2 (1 - \cos \theta_2)$ are found from the geometrical constraints. Therefore, there are three variational parameters: R_b, R_1, θ_1 which minimize the energy in Eq. (3).

Commonly used values of κ=1.4 eV[1] and β corresponding to 40 meV adhesion energy per carbon atom[2,3] suggest an intrinsic length scale $R_0 = \sqrt{\kappa/2\beta} \approx 6.8\,\text{Å}$. Numerical energy minimization from Eq. (1) and (3) using parameters R_0=6.8 Å and

h=3.4 Å leads to the values of the variational radiuses of the left and right bulbs in the *folded wrinkle*: $R_1 \approx 6.5$ Å, $R_3 \approx 4.9$ Å (see Fig. S1 caption) to be in very good agreement with the values found from the DFT optimized geometry of $5-6$ Å[4]. The minimum energy of the *standing collapsed wrinkle* from Eq. (3) as a function of L is given as

$\dfrac{E_{sc}}{\beta R_0} \approx 14.78 - \dfrac{L}{2R_0}$, while minimum energy of the *folded wrinkle* from Eq. (1) is given

by $\dfrac{E_f}{\beta R_0} \approx 27.12 - \dfrac{L}{R_0}$. The equal energy condition $E_{sc} = E_f$ is satisfied for $L_m \approx 24.7R_0$,

which defines a transition height from *standing collapsed wrinkle* to *folded wrinkle* as $R_b + \lambda + R_1\left(1-\cos\theta_1\right) + R_2 \sin\theta_2$, where $\lambda \approx 7.9R_0$ is found from Eq. (4). The height of the *standing wrinkle* at the transition (i.e. the maximum height) is about $12.4R_0 \approx 8.4$ nm, very close to $L_m/2$.

2. Electrostatic modeling of the trilayered folds regions

We model the electrostatics of the graphene fold as a tri-layer graphene system, assuming that the graphene layers are electrically decoupled from one another. Through the Poisson equation, the Dirac point potential in each layer with respect to Fermi energy can be computed as follows,

$$\begin{aligned}
V_2 &= -\tfrac{d_0}{\varepsilon_0} n_3 + V_3 \\
V_1 &= -\tfrac{d_0}{\varepsilon_0}\left(n_2 + n_3\right) + V_2 \\
V_g &= -\tfrac{1}{C_g}\left(n_1 + n_2 + n_3\right) + V_1
\end{aligned} \qquad (5)$$

where V_3 is given a priori. $d_0 = 3.4$Å is the graphene interlayer separation, ε_0 is the free space permittivity, C_g is the back gate capacitance and V_g is the applied gate bias. In Fig. 4a of the main manuscript, the calculated carrier densities assumed a finite electron-hole puddle densities $n_0 = 6.5\times10^{11}$ cm^{-2} estimated from Hall measurements. The fractional carrier population in the graphene layer closest to the gate, i.e. n_1/n where $n = n_1+n_2+n_3$, is closer to unity at larger V_g. On the other hand, the layer densities are more equally

distributed when V_g is biased near the Dirac point. This carrier redistribution within the trilayered graphene system is a consequence of nonlinear screening[4] , and is crucial to explaining our experimental observations.

3. Diffusive transport modeling along/across a graphene fold

We discuss first electronic transport *along* a graphene fold. The effective electrical conductivity σ_{eff} in the diffusive limit can be written as,

$$\sigma_{eff} = \frac{W_f}{W}\left(\sigma_1 + \sigma_2 + \sigma_3\right) + \frac{W - W_f}{W}\sigma \tag{6}$$

where σ_j refers to the electrical conductivity in the jth layer and σ is the electrical conductivity in monolayer graphene i.e. control devices. W_f is the width of the graphene fold, estimated from SEM to be $\approx 0.14\mu$m, and W is the device width. In addition, the electrical conductivity σ as a function of the carrier density n can be determined through Hall measurements. The carrier mean-free-path, $\lambda_{MFP}(n)$, can simply be derived from $\sigma = \frac{4e^2}{\pi h}\sqrt{\pi n}\lambda_{MFP}$ [5]. If each graphene layer in the fold also follows the same $\lambda_{MFP}(n)$ functional relationship, then the respective σ_j are also known. In this case, the calculated σ_{eff} is shown in Fig. 4c of the main manuscript, yielding good agreement. Electronic transport *across* a graphene fold can be modeled in similar fashion, with σ_{eff} written as,

$$\frac{1}{\sigma_{eff}} = \frac{L_f}{L}\left(\frac{1}{\sigma_1} + \frac{1}{\sigma_2} + \frac{1}{\sigma_3}\right) + \frac{L - L_f}{L}\frac{1}{\sigma_0} \tag{7}$$

where L_f is the length of the graphene fold, estimated from SEM to be $\approx 0.14\mu$m, and L is the device length.

4. Quantum transport modeling of *standing collapsed wrinkle*

Here we elaborate on the electronic transport calculation of the *standing collapsed* graphene wrinkle in the main manuscript. We assume that the transport direction is along the armchair direction, as illustrated in Fig. 5a. The Hamiltonian H is described by a nearest neighbor p_z tight-binding model[6] including both in-plane and out-of-plane couplings,

$$H = \sum_i V_i a_i^\dagger a_i + \sum_{<ij>} t_{ij} a_i^\dagger a_j + \sum_{ij} s_{ij} a_i^\dagger a_j \qquad (8)$$

where V_i denote the on-site energy, t_{ij} the in-plane coupling and s_{ij} the out-of-plane coupling. Explicitly, they are expressed as,

$$t_{ij} = \frac{v_{ij} \times p_i}{r_{ij}} \frac{v_{ij} \times p_j}{r_{ij}} \frac{\left(v_{ij} \times p_i\right) \cdot \left(v_{ij} \times p_j\right)}{\left|v_{ij} \times p_i\right| \left|v_{ij} \times p_j\right|} \varepsilon_{pp}^\pi$$

$$s_{ij} = -\alpha\gamma \exp\left(-\frac{r_{ij} - r_p}{\delta}\right) \frac{p_i \cdot v_{ij}}{r_{ij}} \frac{p_j \cdot v_{ij}}{r_{ij}} \qquad (9)$$

where p_i refers to the local out-of-plane vector, v_{ij} is the bond vector and $r_{ij} = \left|v_{ij}\right|$. Parameters $r_p \approx 0.34nm$ refers to the equilibrium graphene interlayer separation, $\gamma \approx 0.119\varepsilon_{pp}^\pi$ is the out-of-plane coupling energy, $\delta \approx 0.185 \times \sqrt{3}r_0$ where $r_0 = 0.142nm$ is the carbon-carbon bond-length and $\alpha \approx 1.4$ is a fitting parameter [6].

Electronic transport across the structure is calculated using the non-equilibrium green function method[5] within the Landauer formalism, assuming periodic boundary condition along the transverse width direction. The transmission function $T\left(k_y, E\right)$ can then be calculated. The finite temperature device conductance can be calculated using,

$$G = \frac{2e^2}{h} \int_{-\infty}^{\infty} \frac{1}{k_B T} \exp\left[\frac{E - \mu}{k_B T}\right] f^2(E) \left[\sum_{k_y} T\left(k_y, E\right)\right] dE \qquad (10)$$

where $f(E)$ is the Fermi Dirac distribution. The resistance associated with the *standing collapsed wrinkle* can then be calculated after subtracting off the quantum contact resistance. In our calculations, we assume that the electrostatic doping of the flat region to be 0.2eV, and undoped in regions which are raised, namely the collapsed bilayer and the structure subtended from it. Temperature is taken to be 300K as per experiments.

5. Temperature dependence of conductivity

The conductivities of the graphene device at 4.2K and 300K are shown in Fig. S3. We observe that the conductivity is nearly unchanged when the temperature is decreased from 300K to 4.2K.

6. Measurements of Hall Mobility

We performed standard Hall measurement to obtain the resistivity tensor and then the conductivities σ_{xx} and σ_{xy}, from which the carrier mobility μ and carrier density n can be extracted.

$$\mu = \frac{1}{B}\frac{\sigma_{xy}}{\sigma_{xx}} \tag{11}$$

$$n = \frac{\sigma_{xx}(1+\mu^2 B^2)}{\mu q} \tag{12}$$

where B is the magnetic field. These quantities are plotted in Fig. S4, obtained at 300K. We emphasize that the extraction method breaks down when the graphene is biased near the Dirac point, the range highlighted in the plot. The observed downturn in the mobility is unphysical, an artifact of the extraction method which ignores the two carrier nature of transport near the Dirac point [7]. Outside this region, the measured mobility clearly shows a decreasing mobility with increasing doping.

7. Dirac point shifts due to folds

The statistical sampling of Dirac voltage for the graphene Hall-bars with and without fold is shown in Fig.S5: (a) across fold vs no fold; (b) along the fold vs no fold. The statistics of Dirac voltage value indicate that the presence of a fold does not lead to significant changes in the Dirac point shifts, hence of the doping level. This indicates that most of the trapped impurities reside in the substrate or the SiO_2-graphene interface.

Reference:

1   Chopra, N. G. *et al.* Fully Collapsed Carbon Nanotubes. *Nature* **377**, 135-138, (1995).
2   Girifalco, L. A. & Lad, R. A. Energy of cohension, compressibility, and the potential energy functions of the graphite system. *Journal of Chemical Physics* **25**, 693-697, (1956).
3   Zacharia, R., Ulbricht, H. & Hertel, T. Interlayer cohesive energy of graphite from thermal desorption of polyaromatic hydrocarbons. *Physical Review B* **69**, (2004).
4   Kuroda, M. A., Tersoff, J. & Martyna, G. J. Nonlinear Screening in Multilayer Graphene Systems. *Physical Review Letters* **106**, 116804, (2011).
5   Datta, S. *Electronic transport in mesoscopic systems*. (Cambridge University Press, 1997).
6   Uryu, S. & Ando, T. Electronic intertube transfer in double-wall carbon nanotubes. *Physical Review B* **72**, 245403, (2005).
7.   Zhu, W., Perebeinos, V., Freitag, M. & Avouris, P. Carrier scattering, mobilities, and electrostatic potential in monolayer, bilayer, and trilayer graphene. *Physical Review B* **80**, 235402, (2009).
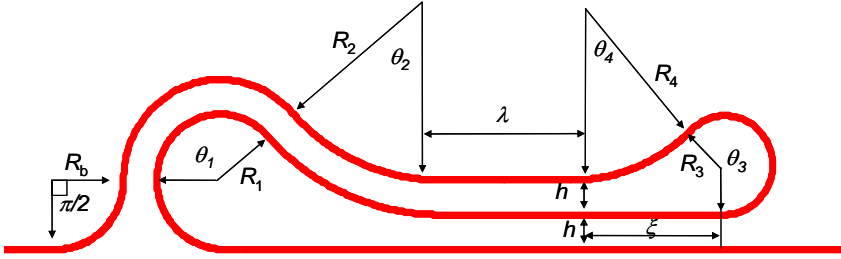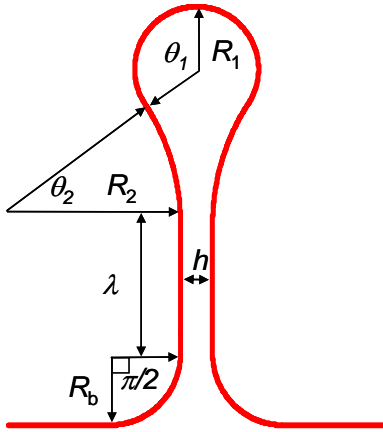
Fig. S1. Schematics of the *folded graphene wrinkle*. The minimum energy from Eq. (1) corresponds to the values of the variational parameters $R_b = R_0$, $R_1 \approx 0.950 R_0$, $R_2 \approx 3.025 R_0$, $\theta_1 \approx 0.764\pi$, $\theta_2 \approx 0.264\pi$, $R_3 \approx 0.714 R_0$, $R_4 \approx 2.555 R_0$, $\theta_3 \approx 1.246\pi$, $\theta_4 \approx 0.246\pi$, where R_0=6.8 Å.

Fig. S2. Schematics of the *standing collapsed graphene wrinkle*. The minimum energy from Eq. (3) corresponds to the values of the variational parameters $R_b = \sqrt{2\pi/(2+\pi)} R_0$, $R_1 \approx 0.967 R_0$, $R_2 \approx 3.401 R_0$, $\theta_1 \approx 0.685\pi$, $\theta_2 \approx 0.185\pi$, where R_0=6.8 Å.
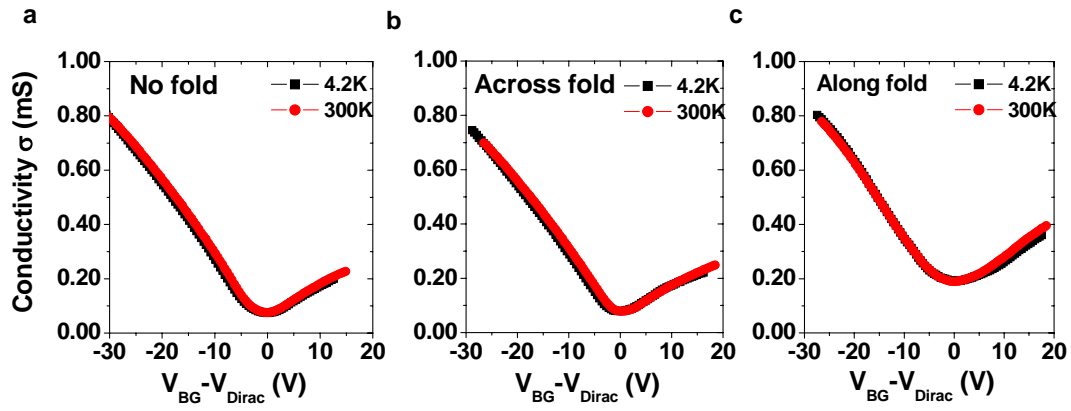
Fig.S3. Conductivity as a function of $V_{BG}-V_{Dirac}$ at 4.2K and 300K for a graphene device (a) with no fold, (b) measured across the fold and (c) along the fold.
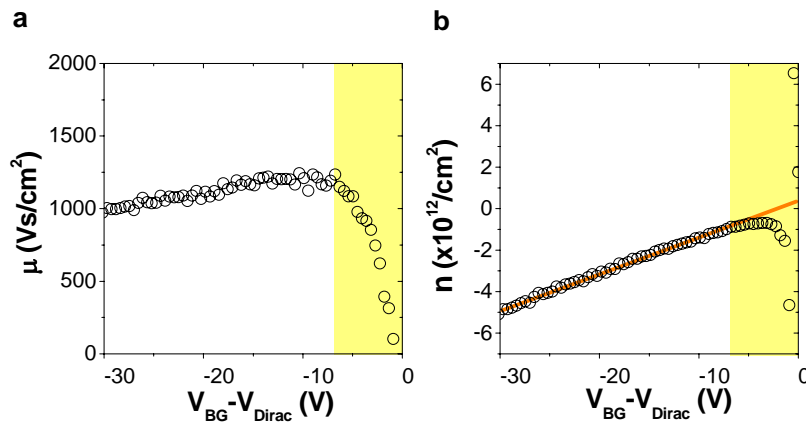

Fig.S4. Extracted (a) Hall mobility and (b) carrier density in graphene at 4K, via the standard Hall measurement procedure.
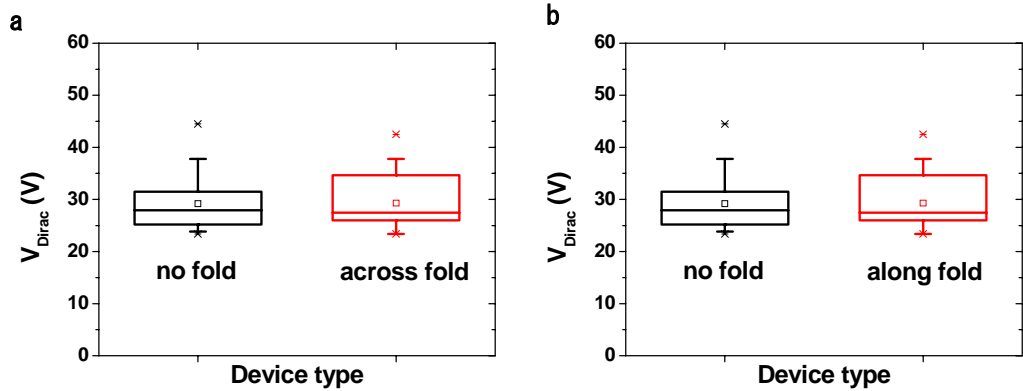
Fig. S5. Statistics of Dirac voltage of graphene Hall-bars (a) across fold vs no fold, and (b) along fold vs no fold. The statistics are based on the data from 42 devices.